In preperation for ApJ Letters
Preprint typeset using LaTeX style emulateapj v. 5/2/11

arXiv:1401.5076v1 [astro-ph.GA] 20 Jan 2014

VARYING [C II]/[N II] LINE RATIOS IN THE INTERACTING SYSTEM BR1202-0725 AT $Z = 4.7$.

R. Decarli[1], F. Walter[1], C. Carilli[2], F. Bertoldi[3], P. Cox[4,5], C. Ferkinhoff[6], B. Groves[1], R. Maiolino[7], R. Neri[4], D. Riechers[6], A. Weiss[8]

In preperation for ApJ Letters

ABSTRACT

We study the properties of the interstellar medium in the interacting system BR1202-0725 at $z = 4.7$ via its [N II] and [C II] fine–structure line emission. This system consists of a QSO, a sub-mm galaxy (SMG), and two Ly-α emitters (LAEs). Such a diversity in galaxy properties makes BR1202-0725 a unique laboratory of star formation and galaxy evolution at high redshift. We present ionized nitrogen ([N II] 205 μm) observations of this system, obtained with the IRAM Plateau de Bure Interferometer. We find no [N II] emission at the quasar location, but tentative [N II] line detections associated with the SMG and one of the LAEs. Together with available ionized carbon ([C II] 158 μm) ALMA observations of this system, we find the following: The [C II]/[N II] luminosity ratio is > 5.5 for the QSO and the SMG, but it is as low as ~ 2 in the LAE, suggesting that, in this source, most of the [C II] emission is associated with the ionized medium (H II regions) rather than the neutral one (PDRs). This study demonstrates the importance of combined studies of multiple fine–structure lines in order to pin down the physical properties of the interstellar medium in distant galaxies.

Subject headings: galaxies: evolution — galaxies: ISM — galaxies: star formation — galaxies: statistics — submillimeter: galaxies — instrumentation: interferometers

1. INTRODUCTION

In local galaxies, optical/UV nebular lines are among the most used diagnostics of the physical properties of the interstellar medium (ISM; see e.g. Baldwin et al. 1981; Vielleux & Osterbrock 1987; Kewley et al. 2006; Groves & Allen 2010). However, these diagnostics are not accessible at high-z, as they are shifted in the mid-infrared regime, where sensitive spectroscopy is out of reach for present instrumentation. The only optical/UV emission line detected at $z > 4$ is hydrogen's Ly-α, which is hard to interpret in terms of ISM physics, due to its resonant nature (see e.g. Yang et al. 2012).

In this context, fine–structure transitions represent key tools to investigate the ISM properties at high-z. With rest-frame wavelengths in the 50–500 μm range, at $z \gtrsim 4$ these lines are redshifted into the (sub-)mm transparent windows of the atmosphere. The most studied fine–structure line is the ionized carbon ([C II]) line at 158 μm, which is now (almost) routinely detected in IR–bright sources at high redshift (Maiolino et al. 2005, 2009; Iono et al. 2006; Walter et al. 2009a; Wagg et al. 2010; Cox et al. 2011; Wagg et al. 2012; Walter et al. 2012; Venemans et al. 2012; Swinbank et al. 2012; Wang et al. 2013; Carilli et al. 2013). Neutral carbon ([C I]) has been reported in about 20 sources at high-z (see Walter et al. 2011; Alaghband-Zadeh et al. 2013). Over the last two years, other fine structure lines have been detected for the first time in high-z galaxies: neutral oxygen [O I] (at 63 and 146 μm, see Coppin et al. 2011; Ferkinhoff et al. 2013), doubly-ionized oxygen [O III] (at 52 and 88 μm, see Ferkinhoff et al. 2010), and ionized nitrogen [N II] (at 122 and 205 μm; see Ferkinhoff et al. 2011; Decarli et al. 2012; Combes et al. 2012; Nagao et al. 2012).

Observations of a combination of these lines provide key diagnostics regarding the physical properties of the atomic and ionized phases of the ISM in galaxies (e.g., the hardness of the UV radiation field, gas temperature and density, mass, metallicity; Petuchowski & Bennett 1993; van der Werf 1999). Ionized nitrogen is of particular interest as its ionization potential (14.53 eV) is slightly above that of hydrogen, so [N II] emission traces the ionized medium, with the ratio between the two forbidden-line transitions of [N II], at 122 and 205 μm, being a direct probe of gas density (in the regime between 10 and 3000 cm^{-3}). The 205 μm [N II] transition has critical density and potential of second ionization that are very close to those of [C II] ($n_c \approx 45$ cm^{-3} and $E_{\rm 2nd\,ion.} \approx 25 - 30$ eV, respectively, if electrons are the main collision partners, as in H II regions). Their flux ratio is thus a diagnostic of the relative abundance of C^+ and N^+ (e.g. Oberst et al. 2006; Walter et al. 2009b; Nagao et al. 2012; Vallini et al. 2013), independently of the hardness of the ionization field. Because the ionization potential of carbon is slightly below the one of hydrogen, the [C II] emission can arise both from H II regions and from the neutral outskirts of dense molecular clouds. Therefore, for a given metallicity, the [C II]–to–[N II] flux ratio can be used to probe the fraction of carbon emission arising from the ionized medium (where both C^+ and N^+ are present) vs. that arising from the neutral phase (where N^+ is suppressed; see, e.g., Oberst et al.

[1] Max-Planck Institut für Astronomie, Königstuhl 17, D-69117, Heidelberg, Germany. E-mail: decarli@mpia.de
[2] NRAO, Pete V. Domenici Array Science Center, P.O. Box O, Socorro, NM, 87801, USA
[3] Argelander Institute for Astronomy, University of Bonn, Auf dem Hügel 71, 53121 Bonn, Germany
[4] IRAM, 300 rue de la piscine, F-38406 Saint-Martin d'Hères, France
[5] ALMA, Chile
[6] Cornell University, 220 Space Sciences Building, Ithaca, NY 14853, USA
[7] Cavendish Laboratory, University of Cambridge, 19 J J Thomson Avenue, Cambridge CB3 0HE, UK
[8] Max-Planck-Institut für Radioastronomie, Auf dem Hügel 69, 53121 Bonn, Germany

2006).

In this Letter, we present first [N II] observations in BR1202-0725, a system of interacting galaxies at $z = 4.695$. This system is of particular interest because it encompasses a QSO (South–East), a sub-mm galaxy (SMG, North–West), and two Ly-α emitters (LAEs, one located between the QSO and the SMG, the other located South-West of the QSO), all accommodated within 10″ on sky (≈ 65 kpc at $z = 4.695$). Fig. 1 shows the *Hubble Space Telescope*/Advanced Camera for Survey i-band image of the field. Given the diversity of galaxy types in such a small region of the sky, BR1202-0725 represents a unique laboratory of star formation and galaxy assembly only ~ 1.2 Gyr after the Big Bang.

The QSO and the SMG are among the brightest, unlensed sources in terms of dust luminosity ($L_{\rm IR} > 10^{13}$ $L_\odot$). The optical/NIR images of the QSO are completely dominated by the nuclear light, which overwhelms the host galaxy starlight (see Fig. 1). The SMG is barely detected at optical/NIR wavelengths, due to heavy dust obscuration. All the companion galaxies are clearly detected in sensitive *HST* and ground–based broad–band observations of the rest–frame UV/optical stellar continuum. The LAEs are also clearly detected in dedicated narrow–band observations encompassing the Ly-α line (Hu et al. 1996) and in spectroscopic observations of this system (Ohyama et al. 2004; Williams et al. in prep.).

Thanks to its enormous IR luminosity, BR1202-0725 has been long studied at (sub-)mm wavelengths. Multiple CO transitions (1-0, 2-1, 4-3, 5-4, 7-6) have been detected (Omont et al. 1996; Carilli et al. 2002; Riechers et al. 2006; Salomé et al. 2012), together with neutral and ionized carbon fine structure lines (Iono et al. 2006; Salomé et al. 2012). Wagg et al. (2012) and Carilli et al. (2013) presented Atacama Large Millimeter Array (ALMA) observations of the [C II] emission in BR1202-0725. The [C II] emission is clearly detected in the QSO and the SMG. Interestingly, they also reported continuum and tentative line detections associated with LAE–2, although only part of the line width fell into the ALMA bandpass. A [C II] detection is also reported at the position of LAE–1. These observational efforts have provided us with a plethora of probes of the neutral and molecular gas in BR1202-0725. The data presented here allow us to complement this information by probing the ionized phase of the ISM through observations of the [N II] line.

The Letter is structured as follows: §2 describes our [N II] observations of BR1202-0725. §3 presents our results, and compares them with the results of [C II] studies. Conclusions are drawn in §4. Through the Letter we assume a ΛCDM cosmology, with $H_0 = 70$ km s^{-1} Mpc^{-1}, $\Omega_{\rm m} = 0.3$, and $\Omega_\Lambda = 0.7$.

2. OBSERVATIONS

We observed BR1202-0725 with the IRAM Plateau de Bure Interferometer (PdBI). We targeted the [N II] 205 μm transition ($\nu_0 = 1461.132$ GHz). The tuning frequency was 256.564 GHz (WideX band 3), corresponding to z([N II])= 4.695. The pointing center was set to RA=12:05:23.100, Dec=-07:42:33.00, J2000.0). The primary beam of PdBI can be described by a Gaussian profile with full width at half maximum (FWHM) = $47.3'' \times (100/\nu)$, where ν is the observing frequency in GHz. At the tuning frequency of our observations, the primary beam is 18.4″ in diameter (see Fig. 1). Observations were obtained on January 8, 2013, with the array in compact, 6–antenna configuration (6Cq). Baselines ranged between 18.0 and 176.0 m. The quasars 3C84 and 1055+018 were observed as flux calibrators. The quasar 3C273 served as phase and amplitude calibrator. We processed our data using the most recent version of the GILDAS software. The receiver operated in the upper sideband, with a typical system temperature of 300 K. The final cube consists of 5280 visibilities, corresponding to 4.4 hr on source (6-antennas equivalent).

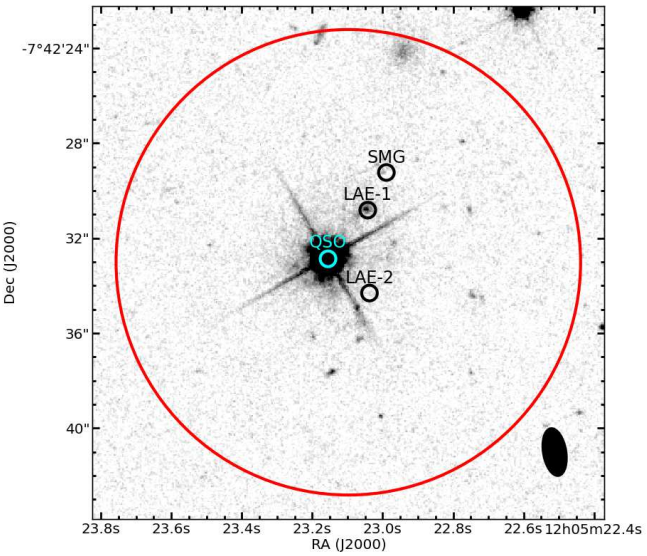

FIG. 1.— Map of BR1202-0725 as observed with *HST*/ACS (F775W filter, i-band). The various components of this system are labeled. The beam of our [N II] observations (2.0″ × 0.9″) is shown as a black ellipse in the bottom–right corner. The big circle marks the primary beam of PdBI at the observed frequency (18.4″).

We imaged the cube using the GILDAS suite mapping. Natural weighting was adopted. The beam size is 2.0″ × 0.9″ (~ 13 kpc ×6 kpc at $z = 4.695$). We estimate an rms of 1.3 mJy beam^{-1} per 100 km s^{-1} channel. We applied Hogbom cleaning down to 2-σ per channel in a box encompassing all the individual components of BR1202-0725.

We compare our [N II] observations with the [C II] data presented in Wagg et al. (2012) and Carilli et al. (2013). [C II] data were collected with the Atacama Large Millimeter Array (ALMA) during science testing and verification in January 2012. The observations cover 2 GHz of bandwidth, centered at 333.9 GHz, i.e., encompassing the [C II] 158 μm emission of the QSO and the SMG. The resolution of these data is 1.2″ × 0.8″.

3. RESULTS

3.1. *[N II] 205 μm in BR1202-0725*

Fig. 2 shows the continuum–subtracted [N II] and [C II] spectra of the galaxies in the BR1202-0725 system. The continuum levels have been measured by averaging line–free channels in the cubes (see Table 1), and are consistent with the SED study presented in Wagg et al. (in prep.). No [N II] emission is found to be associated with the QSO. A faint [N II] line (with possibly two emis-

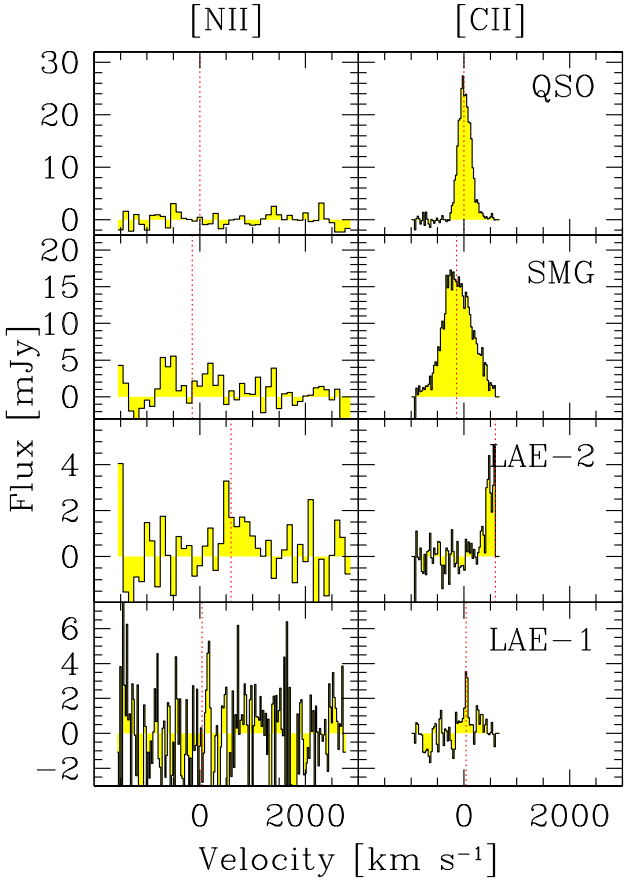

FIG. 2.— Comparison between the continuum-subtracted spectra of [N II] (left) and [C II] (right; Wagg et al. 2012; Carilli et al. 2013) in BR1202-0725. These panels have the same scales, to emphasize the wide range of [C II]/[N II] flux ratios probed with our observations. Vertical lines highlight the peak positions of the lines, as derived by Carilli et al. (2013). No line is detected in the QSO. A tentative, double-horned [N II] line detection is found at the position of the SMG. A tentative line is detected at the position of both the Ly-α emitters.

sion peaks) is detected at the position of the SMG. The integrated line flux is 2.7 ± 0.5 Jy km s^{-1}. The line emission is marginally resolved along the West–East axis, consistently with what observed in the CO and [C II] emission (Salomé et al. 2012; Wagg et al. 2012; Carilli et al. 2013).

LAE–2 shows [N II] emission with line flux of 1.10 ± 0.35 Jy km s^{-1}, and a width of 370 km s^{-1}. The [N II] emission from this galaxy matches the line profile observed for the [C II] line, although only the blue wing of the [C II] line has been covered by the ALMA observations presented in Wagg et al. (2012) and Carilli et al. (2013). On the other hand, the [N II] detection in LAE–1 is only very marginal. The tentative line shows a very narrow profile (FWHM$\approx$50km s^{-1}) similar to the [C II] line, which is however offset in velocity by the same amount. The [N II] line flux is 0.28 ± 0.12 Jy km s^{-1}, corresponding to a ~ 2.5-σ nominal detection. Future observations with ALMA are necessary to confirm this tentative detection. Table 1 summarizes the velocity offsets among the various components and the continuum and line parameters (1461 GHz continuum; width, flux and luminosity of the [N II] line) observed in our study.

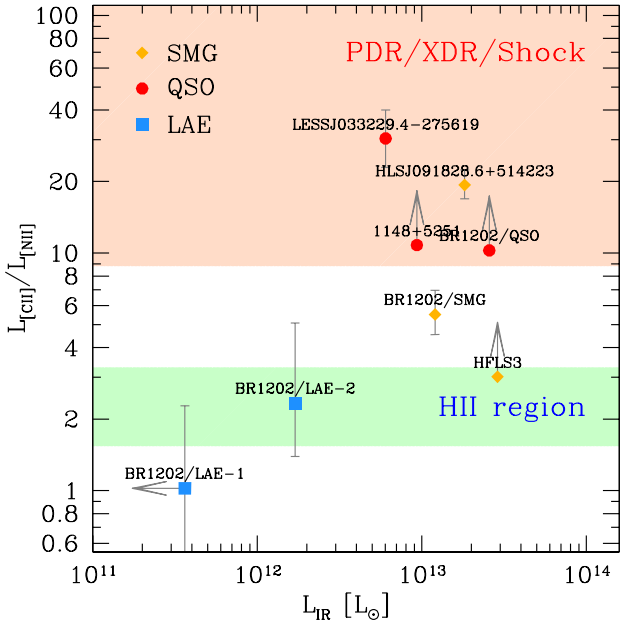

FIG. 3.— The luminosity ratio of [C II] and [N II] as a function of IR luminosity, as measured in all the high-z galaxies for which [C II] has been detected, and sensitive [N II] limits are available. Symbols are coded based on the galaxy type. For LAE–2 in BR1202-0725, we have integrated the fluxes of both [C II] and [N II] only in the velocity range observed in both the lines (see Fig. 2). The ratio for LAE-1 would be a lower limit if follow-up observations were not to confirm our tentative detection.

3.2. *The [C II]/[N II] ratio*

Wagg et al. (2012) and Carilli et al. (2013) reported strong [C II] detections in the QSO and the SMG. LAE–1 shows a very narrow [C II] line (FWHM$\approx$50 km s^{-1}). [C II] line is also reported in LAE–2, though in this case the ALMA observations only covered part of the line profile (see Fig. 2).

The comparison between [N II] and [C II] emission in the various components of BR1202-0725 reveals highly diverse properties in the properties of the interstellar medium in the various galaxies. We follow Oberst et al. (2006) in order to estimate the fraction of [C II] associated with the ionized medium (stellar H II regions), in contrast with the neutral surface of dense photon-dominated regions (PDRs) in the outskirt of molecular clouds, or other environments (e.g., X-ray dominated regions, XDRs Meijerink et al. 2007; shocks Meijerink et al. 2010; Appleton et al. 2013; etc). In a H II region with fixed metallicity, the expected ratio of the two lines is practically independent of the gas density. Assuming $n(\mathrm{N}^+)/n_\mathrm{e} = 7.9 \times 10^{-5} = 0.56\, n(\mathrm{C}^+)/n_\mathrm{e}$ (Savage & Sembach 1996), we expect a ratio of line luminosities $L([\mathrm{C\,II}])/L([\mathrm{N\,II}])) \approx 2$. In the LAEs, the observed [C II]–to–[N II] ratio is consistent with unity, thus suggesting that these lines are associated with a purely ionized medium. On the other hand, the [C II]–to–[N II] ratio in the SMG and, most of all, in the QSO, is much higher (see Table 1).

In Fig. 3 we plot the [C II]–to–[N II] ratio as a function of IR luminosity for the various components of BR1202-0725, and for the few galaxies at $z > 1$ for which both [C II] has been detected, and deep [N II] 205

TABLE 1
[N II] line parameters in the BR1202-0725 system. (1) Galaxy ID. (2) Continuum flux at 1461 GHz (rest frame). (3) Line peak velocity, with respect to the peak of [C II] emission in the QSO (see Fig. 2). (4) [N II] 205 μm line flux. (5) [N II] FWHM. (6–7) [N II] line luminosity. (8) [C II]–to–[N II] luminosity ratio. (9) IR luminosity, taken from Carilli et al. (2013). Typical uncertainties in the IR luminosities are $\sim 20\%$. In case of non-detections, 3-σ limits are reported.

Galaxy	$F_{\rm cont}$ (mJy)	Δv (km s^{-1})	$F_{\rm line}$([N II]) (Jy km s^{-1})	FWHM (km s^{-1})	L'([N II]) (10^9 K km s^{-1} pc^2)	L([N II]) (10^8 L$_\odot$)	L([C II])/L([N II])	log $L_{\rm IR}$ (L$_\odot$)
(1)	(2)	(3)	(4)	(5)	(6)	(7)	(8)	(9)
QSO	8.2 ± 0.3	—	-0.04 ± 0.31	—	< 4.7	< 4.6	> 10.3	13.41
SMG	7.8 ± 0.5	-195 ± 160	2.69 ± 0.53[a]	940^{+260}_{-300}	13.5 ± 2.6[a]	13 ± 3[a]	$5.5^{+1.5}_{-1.0}$	13.08
LAE-1	< 0.7	137 ± 27	0.28 ± 0.12	50^{+70}_{-20}	1.4 ± 0.6	1.4 ± 0.6	$1.0^{+1.3}_{-0.5}$	< 11.56
LAE-2	0.7 ± 0.3	673 ± 197	1.10 ± 0.35	370^{+50}_{-170}	5.5 ± 1.8	5.5 ± 1.8	—	12.23
LAE-2[b]	0.7 ± 0.3	—	0.39 ± 0.19	—	1.9 ± 0.9	1.9 ± 0.9	$2.3^{+2.7}_{-0.9}$	12.23

[a]Not corrected for the marginally resolved emission
[b]Computed in the velocity range where the [C II] is also covered (see Fig. 2).

μm observations have been reported in the literature (Walter et al. 2009a; Combes et al. 2012; Nagao et al. 2012; Riechers et al. 2013). These sources are either SMGs or QSO host galaxies with bright IR emission ($L_{\rm IR} \sim 10^{13}$ L$_\odot$). The LAEs in our study have substantially lower IR luminosity ($\sim 10^{12}$ L$_\odot$ in LAE–2; $< 3 \times 10^{11}$ L$_\odot$ in LAE–1). Moreover, their [C II]–to–[N II] ratio is substantially lower than typically observed in IR–bright SMGs and QSOs at high–z, and is consistent with the range of values expected for H II–region conditions (shaded green area). On the other side, the majority of the IR–bright sources studied so far have high [C II]–to–[N II] ratios. This suggests that there is additional [C II] emission that may be arising from the *neutral* medium in the outskirts of dense molecular regions (PDR–like) or from extended XDRs, where [N II] is not present (red shaded area in Fig. 3). In particular, in the QSO, the observed ratio is $\gtrsim 3$ times higher than what predicted in the most conservative H II–region scenario, thus suggesting that $\lesssim 33\%$ of the [C II] in this source is emitted in the ionized phase of the ISM. The global ratio observed in the SMG is lower, ≈ 5.5, still too high for H II regions. However, the different profiles of the [C II] and [N II] lines in this source suggest that the picture is more complex, and that we are probably witnessing a composite source in which both H II regions and dense molecular clouds play important roles. Deeper data at higher spatial resolution and significantly higher signal-to-noise with ALMA will allow us to perform a velocity- and spatially–resolved study of the [C II]–to–[N II] ratio, thus disentangling the role of each component.

4. CONCLUSIONS

We have presented first [N II] 205 μm observations in BR1202-0725, an IR–bright system of interacting galaxies at $z \approx 4.7$. The system consists of a QSO, an SMG, and two LAEs. We report [N II] detections in the SMG and in the LAE–2. We combine the observations of the [N II] with previously published [C II] observations. The [C II]–to–[N II] luminosity ratios span over one order of magnitude, being < 5 in the LAEs, and > 5 in the SMG and in the QSO. We use this line ratio to put constraints on the fraction of [C II] associated with the *ionized* phase of the ISM. The LAEs are well within the parameter space of H II regions. On the other hand, the [C II] emission associated with the neutral phase is high in the SMG and, most of all, in the QSO. This is the first time that the relative importance of the ionized vs neutral phases of the ISM can be directly compared in high-z galaxies.

Deeper observations of this system, in particular using the Atacama Large Millimeter Array, are crucial in order to confirm the tentative [N II] detections reported here. In addition, observations of other fine-structure lines (e.g., [O III] and [O I]) will allow us to expand our analysis to different regimes (e.g., the highly–ionized medium) and to put first constraints on other parameters (e.g., metallicity) in this unique laboratory of star formation in the early universe.

ACKNOWLEDGMENTS

This work is based on observations carried out with the IRAM Plateau de Bure Interferometer. IRAM is supported by INSU/CNRS (France), MPG (Germany) and IGN (Spain). This research made use of Astropy, a community-developed core Python package for Astronomy (the Astropy collaboration 2013). Support for RD was provided by the DFG priority program 1573 "The physics of the interstellar medium".

REFERENCES

Alaghband-Zadeh S., Chapman S.C., Swinbank A.M., Smail I., Danielson A.L.R., Decarli R., Ivison R.J., Meijerink R., Weiß A., van der Werf P., 2013, MNRAS, 435, 1493
Appleton P.N., Guillard P., Boulanger F., Cluver M.E., Ogle P., Falgarone E., Pineae de Forêts G., O'Sullivan E., 2013, ApJ, 777, 66
The Astropy collaboration: Robitaille T.P., Tollerud E.J., Greenfield P., Droettboom M., Bray E., Aldcroft T., Davis M., Ginsburg A., et al., 2013, A&A, in press (arXiv:1307.6212)
Baldwin J.A., Phillips M.M., Terlevich R., 1981, PASP, 93, 5
Benford D.J., 1999, PhD Thesis, Caltech
Carilli C.L., Kohno K., Kawabe R., Ohta K., Henkel C., Menten K.M., Yun M.S., Petric A., Tutui Y., 2002, AJ, 123, 1838
Carilli C.L., Riechers D., Walter F., Maiolino R., Wagg J., Lentati L., McMahon R., Wolfe A., 2013a, ApJ, 763, 120
Carilli C.L. & Walter F., 2013b, ARA&A, 51, 105
Combes F., Rex M., Rawle T.D., Egami E., Boone F., Smail I., Richard J., Ivison R.J., et al., 2012, A&A, 538, L4

Coppin K.E.K., Danielson A.L.R., Geach J.E., Hodge J.A., Swinbank A.M., Wardlow J.K., Bertoldi F., Biggs A., Brandt W.N., et al., 2012, MNRAS, 427, 520
Cox P., Krips M., Neri R., Omont A., Güsten R., Menten K.M., Wyrowski F., Weiss A., et al., 2011, ApJ, 740, 63
Decarli R., Walter F., Neri R., Bertoldi F., Carilli C., Cox P., Kneib J.P., Lestrade J.F., Maiolino R., Omont A., et al. 2012, ApJ, 752, 2
Ferkinhoff C., Hailey-Dunsheath S., Nikola T., Parshley S.C., Stacey G.J., Benford D.J., Staguhn J.G., 2010, ApJ, 714, L147
Ferkinhoff C., Brisbin D., Nikola T., Parshley S.C., Stacey G.J., Phillips T.G., Falgarone E., Benford D.J., Staguhn J.G., Tucker C.E., 2011, ApJ, 740, L29
Ferkinhoff C., Brisbin D., Parshley S.C., Nikola T., Stacey G.J., Schoenwald J., Higdon J.L., Higdon S.J.U., Verma A., et al. 2013, ApJ, in press (arXiv:1311.1515)
Groves B.A., Allen M.G., 2010, New Ast. 15, 614
Hu E.M., McMahon R.G., Egami E., 1996, ApJ, 459, L53
Iono D., Yun M.S., Elvis M., Peck A.B., Ho P.T.P., Wilner D.J., Hunter T.R., Matsushita S., Muller S., 2006, ApJ, 645, L97
Ivison R.J., Harrison A.P., 1996, A&A, 309, 416
Kewley L.J., Groves B., Kauffmann G., Heckman T., 2006, MNRAS, 372, 961
Krips M., Peck A.B., Sakamoto K., Petitpas G.B., Wilner D.J., Matsushita S., Iono D., 2007, ApJ, 671, L5
Maiolino R., Cox P., Caselli P., Beelen A., Bertoldi F., Carilli C.L., Kaufman M.J., Menten K.M., Nagao T., Omont A., et al., 2005, A&A, 440, L51
Maiolino R., Caselli P., Nagao T., Walmsley M., De Breuck C., Meneghetti M., 2009, A&A, 500, L1
Meijerink R., Spaans M., Israel F.P., 2007, A&A, 461, 793
Meijerink R. Spaans M., Loenen A.F., van der Werf P.P., 2011, A&A, 525, 119
Nagao T., Maiolino R., De Breuck C, Caselli P., Hatsukade B., Saigo K., 2012, A&A, 542, L34
Oberst T.E., et al. 2006, ApJ Letters, 652, 125
Ohyama Y., Taniguchi Y., Shioya Y., 2004, AJ, 128, 2704
Omont A., McMahon R.G., Cox P., Kreysa E., Bergeron J., Pajot F., Storrie-Lombardi L.J., 1996, A&A, 315, 1
Petuchowski S.J., & Bennett C.L., 1993, ApJ, 405, 591
Riechers D.A., Walter F., Carilli C.L., Knudsen K.K., Lo K.Y., Benford D.J., Staguhn J.G., Hunter T.R., et al. 2006, ApJ, 650, 604
Riechers D.A., Bradford C.M., Clements D.L., Dowell C.D., Pérez-Fournon I., Ivison R.J., Bridge C., Conley A., et al. 2013 Nature, 496, 329
Salomé P., Guélin M., Downes D., Cox P., Guilloteau S., Omont A., Gavazzi R., Neri R., 2012, A&A, 545, 57
Savage B.D., & Sembach K.R., 1996, ARA&A, 34, 279
Swinbank A.M., Karim A., Smail I., Hodge J., Walter F., Bertoldi F., Biggs A.D., de Breuck C., Chapman S.C., Coppin K.E.K., et al. 2012, MNRAS, 427, 1066
Vallini L., Gallerani S., Ferrara A., Baek S., 2013, MNRAS, 433, 1567
van der Werf P.P., 1999, Highly Redshifted Radio Lines, 156, 91
Venemans B.P., McMahon R.G., Walter F., Decarli R., Cox P., Neri R., Hewett P., Mortlock D.J., Simpson C., Warren S.J., 2012, ApJ, 751, L25
Vielleux S., Osterbrock D.E., 1987, ApJ S., 63, 295
Yang Y., Decarli R., Dannerbauer H., Walter F., Weiß A., Leipski C., Dey A., Chapman S.C., et al. 2012, ApJ, 744, 178
Wagg J., Carilli C.L., Wilner D.J., Cox P., De Breuck C., Menten K., Riechers D.A., Walter F., 2010, A&A, 519, L1
Wagg J., Wiklind T., Carilli C.L., Espada D., Peck A., Riechers D., Walter F., Wootten A., Aravena M., et al. 2012, ApJ, 752, L30
Wagg J., Carilli C.L., Aravena M., Cox P., Lentati L., Maiolino R., McMahon R.G., Riechers D., et al. 2014, in prep.
Walter F., Weiss A., Riechers D.A., Carilli C.L., Bertoldi F., Cox P., Menten K.M., 2009a, ApJ, 691, L1
Walter F., Riechers D., Cox P., Neri R., Carilli C., Bertoldi F., Weiss A., Maiolino R., 2009b, Nature, 457, 699
Walter F., Weiss A., Downes D., Decarli R., Henkel C., 2011, ApJ, 730, 18
Walter F., Decarli R., Carilli C., Bertoldi F., Cox P., da Cunha E., Daddi E., Dickinson M., et al. 2012, Nature, 486, 233
Wang R., Wagg J., Carilli C.L., Walter F., Lentati L., Fan X., Riechers D.A., Bertoldi F., Narayanan D., et al. 2013, ApJ, 773, 44
Williams R.K., et al. 2014, MNRAS, in prep.